Chemical kinetics of bean straw biofuel pyrolysis using maximum volatile release method

Wei Chen[*,†], **Kalyan Annamalai**[**], **Jiafeng Sun**[**], **and Yuming Chen**[*]

*School of Electronic Power Engineering, China University of Mining and Technology Xuzhou, Jiangsu 221008, China
**Department of Mechanical Engineering, Texas A&M University, College Station, TX 77840, U.S.A.

Abstract−Maximum volatile release (MVR) methods, including single point (MVR-S) and multiple (MVR-M) points, are proposed to extract the kinetics used to predict the fuel bean straw pyrolysis process. The simulation results were compared to those of the distributed activation energy model (DAEM). For the TGA (thermogravimetric analysis) experiments, fuels were heated from ambient temperature to 1,173 K at the heating rates of 10, 20, 40, 60, 80 K min^{-1}, and the corresponding maximum volatile release points were obtained. For the MVR-S method, both the activation energy (E) and pre-exponential factor (B) increased with increasing heating rates. For the pyrolysis weight loss process, the DAEM showed best agreement with the experimental data, followed by the MVR-M, and then the MVR-S method. However, for weight loss rate prediction, MVR-S method had the best match with the experimental data, whereas the DAEM and MVR-M method generated more errors.

Keywords: Pyrolysis, Torrefaction, Volatile Matter, Kinetics, Activation Energy

INTRODUCTION

The strong demand for fossil fuels and the increasing fuel price has directed significant attention to renewable fuels such as agricultural biomass as alternative fuels to decrease greenhouse gas emission. A large amount of agricultural waste, such as feedlot waste and mesquite, has been used as feedstock for biogas and liquid biofuel production [1,2]. Combustion, gasification, pyrolysis, and torrefaction are the main thermochemical conversion technologies to convert biomass fuels into more useful energy sources. Among these thermochemical technologies, pyrolysis is the first step to understand combustion, gasification, and torrefaction. However, the pyrolysis of biomass is very complex with competitive and concurrent reactions, and the exact mechanism needs further detailed investigation [3]. TGA often has been used to study fuel pyrolysis owing to its simplicity and straightforward pyrolysis behavior [4]. By studying the coffee ground and Douglas fir mixture pyrolysis characteristics, it was found that the synergetic effect of biomass mixture can lower the fuel activation energy [5]. Recently, the kinetics of pyrolysis was used to predict mesquite torrefaction upper limit temperature (T_{max}, corresponding to the temperature where the maximum volatile release rate occurred) to avoid significant weight loss [6].

The single reaction model and the distributed activation energy model are well known and the most common methods used to simulate biomass fuel pyrolysis [7]. In the single reaction model, the activation energies (E) of different biomasses are predicted by using the direct or modified Arrhenius plot method [8-10]. However, this method does not appropriately consider heterogeneous

chemical reactions and interactions during the pyrolysis and has a restriction in the simulation [11]. Tran et al. found that the extracted kinetics obtained by the single reaction model was not realistic and not suitable for simulating stump biomass pyrolysis [12]. Cardoso et al. also found that single reaction model was not good for tobacco waste and sorghum bagasse pyrolysis [13]. Similar results were also reported by others [14,15]. Biomass fuels consist of several components, including hemicellulose, cellulose and lignin. Since the activation energy is related to bond energy, which varies widely among biomass fuels having multiple components, it can be assumed that the pyrolysis process consists of an infinite number of reactions proceeding in parallel with activation energy E ranging from 0 to infinity. The distributed activation energy model (DAEM) considers a large number of reactions occurring inside the biomass when it is heated. Thus, DAEM was considered to be more accurate than other reaction models [16,17].

DAEM was first proposed by Pitt et al. in 1962 [18]. Anthony et al. developed a more general first-order parallel reaction model for lignite and bituminous coals in 1976 [19]. Recently, DAEM has not only been used to study the degradation of coal [20-22], but also to describe the pyrolysis kinetics of different biomass [23,24] and oil shale [25]. Based on the Anthony theory, different DAEMs were further developed to better describe the fuel pyrolysis process. Junpirom et al. [26] developed two-component models (hemicellulose and lignin) for longan seed biomass. Both the reactions were assumed to proceed simultaneously. Cai et al. developed three-parallel-reaction model (e.g., hemicellulose, cellulose, and lignin) for describing rice straw pyrolysis and found that the model used to describe the standard deviations of the activation energy distributions exhibited was less sensitive for all the pseudocomponents [27]. Braun et al. developed the nth-order DAEM and applied it to the pyrolysis of sintering of hydroxyapatite [28,29]. These DAEMs did not consider temperature dependency of frequency factor. Mani

et al. and Cai et al. developed the DAEM model by considering temperature dependent pre-exponential factor to improve the accuracy of the model [30,31]. Later, Cai et al. further developed the nth-order distributed activation energy model by considering the effects of various parameters including the dependence of frequency factor on temperature [31,32]. Although DAEM well predicted the biomass pyrolysis volatile release weight lost process, it did not estimate the volatile release rate well, especially at the T_{peak} point [6]. Chen et al. first proposed a maximum volatile matter release single point method (MVR-S) for mesquite pyrolysis [6]. In this method, kinetic parameters such as activation energy and pro-exponential factor are extracted from the maximum volatile release rate point, and this model predicts the volatile release rate well. No other data is available in the literature on the maximum volatile matter method for predicting biomass pyrolysis volatile release rate.

Our objective was to develop a maximum volatile release method, including a new proposed multiple-point method (MVR-M) to predict the bean straw pyrolysis process. The simulation results on the weight loss behavior and volatile release rate by the DAEM, MVR-S, and MVR-M methods were compared to the experimental data, and the accuracy of each method was evaluated.

EXPERIMENTAL

Soybean (Glycine max) straw samples, species of legume native to East Asia, were harvested from the northern part of Jiangsu Province, China. Leaves and small twigs of the samples were removed from the branches before grinding. Before the experiment, ~100 g of samples was first crushed into small-sized powder. Then, these powders were sieved by two standard screens corresponding to Sauter mean diameter of 200 (75 μm) and 320 (45 μm). The particles of selected sizes (45-75 μm) were collected for TGA study.

TGA and differential thermal analyses (DTA) were conducted on the bean straw using a TGA-DTA instrument (LABSYS evo, Setaram). In each experiment, ~10-12 mg samples was heated at heating rates of 10, 20, 40, 60, and 80 K min^{-1} from ambient temperature to 1,170 K in an inert environment using N_2 as the purging gas. The mass (m) of the fuel as a function of sample temperature (T) was recorded for the trace.

METHODS

1. First-order Global Pyrolysis Reaction Equation

The first-order one step single-reaction model offers a simple mathematical description of the pyrolysis (or thermal decomposition) of biomass. The rate of devolatilization for a first-order pyrolysis of dry ash free biomass can be expressed by the following equation [33].

$$\frac{dm_v}{dt} = -Bm_v \exp\left(\frac{-E}{RT}\right) \tag{1}$$

where m_v is the mass of the volatiles remaining in the sample, B is the pre-exponential rate constant (min^{-1}), E is the activation energy (kJ/kmol), and R is the ideal gas constant (8.314 kJ/kmol K).

Because the heating rate (dT/dt=β) is constant, Eq. (1) can be simplified in terms of exponential integrals as represented by the following equation:

$$\ln\left(\frac{m_v}{m_{v0}}\right) = \frac{B}{\beta}\left(\frac{E}{R}\right) \cdot \left\{\frac{E_2(X)}{X} - \frac{E_2(X_0)}{X_0}\right\} \tag{2}$$

where X=(E/RT). Approximations for $E_2(X)$ can be found in reference [33].

2. Distributed Activation Energy Model

The pyrolysis process was assumed to consist of an infinite number of complex reactions proceeding in parallel with E ranging from 0 to infinity [19]. If $\delta m_{V,E}$ is the mass change within a short period of time dt having an activation energy between E and E+dE, the rate of liberation of volatiles for the first-order pyrolysis can be written according to Eq. (1) where m_v is replaced by δm_V. Assuming the Gaussian distribution of the activation energy, the fraction of the initial total volatile mass having the activation energy between E and E+dE can be expressed as:

$$\frac{\delta m_{v,E,0}}{m_{v,0}} = f(E)dE \tag{3}$$

where $f(E) = \frac{1}{\sigma\sqrt{2\pi}} \exp\left(-\frac{(E-E_m)^2}{2\cdot\sigma^2}\right) \tag{4}$

and $\int_0^\infty f(E)dE = 1 \tag{5}$

where E_m is the mean activation energy, and σ is the standard deviation of activation energy. The Gaussian distribution indicates that 1% mass has activation energy of E<E_m-2.3 σ; these E values refer to low activation energy components of the volatiles. The detailed calculation process for E_m and σ of this method was described by Chen et al. [6].

3. Maximum Volatile Release Method (MVR)

The maximum volatile release method single point was first applied to simulate the amount of volatile released and the volatile release rate of mesquite pyrolysis [6]. The maximum volatile release rate of volatiles and the corresponding temperature T_{max} can also be determined by differentiating Eq. (1) with T and setting $d^2m_v/dT^2=0$; solving for T_{max}, the kinetic constants B and E were determined [6]. Setting T=T_{max} in Eqs. (1) and (2), $\{dm_v/dT\}_{max}$ and $\{m_v/m_{v0}\}_{T=Tmax}$ were obtained, leading to the following three relationships.

$$B = \left(\frac{E\cdot\beta}{R\cdot T_{max}^2}\right)\cdot\exp\left(\frac{E}{R\cdot T_{max}}\right) \tag{6}$$

$$\left(\frac{df}{dT}\right)_{max} = -\frac{1}{X_{max}T_{max}}\exp\left[X_{max}^2\cdot\exp(X_{max})\left(\frac{E_2(X_0)}{X_0} - \frac{E_2(X_{max})}{X_{max}}\right)\right] \tag{7}$$

$$\ln\left(\frac{m_v}{m_{v0}}\right)_{X=X_{max}} = \frac{B}{\beta}\left(\frac{E}{R}\right)\cdot\left\{\frac{E_2(X_{max})}{X_{max}} - \frac{E_2(X_0)}{X_0}\right\} \tag{8}$$

where X_{max} is (E/RT$_{max}$).

3-1. Single Point Method (MVR-S)

Knowing T_{max} and $(df/dT)_{max}$ from the TGA data, the two unknowns, E and B, can be solved from Eqs. (6) and (7), and $(m_v/m_{v0})_{X=X_{max}}$ can be computed from Eq. (8). In this study, T_{max} and $\{dm_v/dT\}_{max}$ at different heating rates were obtained from the TGA curves,

and E and B were calculated and compared by using Eqs. (6)-(8).

3-2. Multiple Point Method (MVR-M)

Taking logarithm of Eq. (6) leads to the following equation:

$$\ln B = \ln\left(\frac{\beta}{T_{max}^2}\right) + \ln\left(\frac{E}{R}\right) + \left(\frac{E}{R \cdot T_{max}}\right) \tag{9}$$

where T_{max} is a function of the heating rate β. Higher heating rate results in lower volatile loss because of the shorter residence time and hence more volatile matter remains in the solid; thus, T_{max} occurs at higher temperature at higher heating rates. The experiments were repeated at different heating rates and a series of values for T_{max}, the slope in the plot of $\ln(\beta/T_{max}^2)$ versus $1/T_{max}$, yields
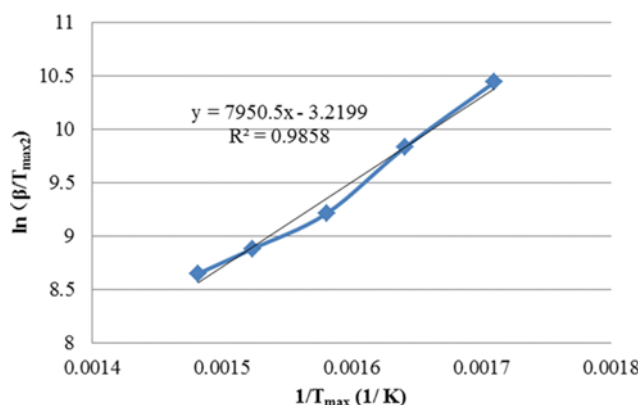

Fig. 1. $\ln(\beta/T_{max}^2)$ versus $1/T_{max}$ at different heating rates.

Table 1. Bean straw proximate and ultimate analysis

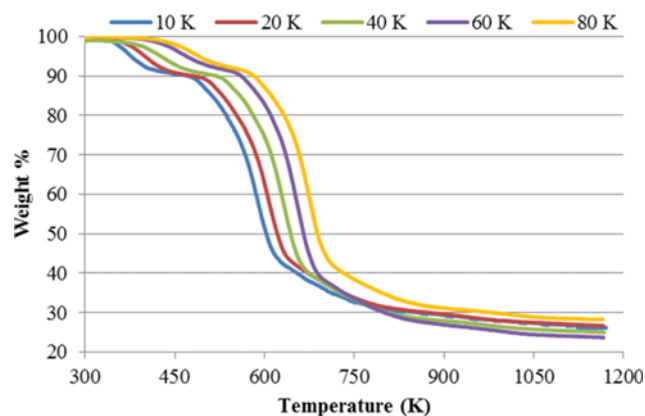| As received	
Moisture	9.5
Ash	6.11
VM	70.2
FC	14.18
Carbon	37.65
Oxygen	39.98
Hydrogen	5.61
Nitrogen	0.85
Sulfur	0.3
HHV (kJ/kg)	15408.78
Dry, Ash Free	
Moisture	0
Ash	0
VM	83.19
FC	16.81
Carbon	44.61
Oxygen	47.38
Hydrogen	6.65
Nitrogen	1.01
Sulfur	0.35
HHV (kJ/kg)	18259.25
Chemical formula	$CH_{1.7726}O_{0.7972}N_{0.0194}S_{0.0029}$

Fig. 2. Bean straw TGA weight loss curves at different heating rates.

E/R value. In this study, the curve of $\ln(\beta/T_{max}^2)$ versus $1/T_{max}$ for the bean straw pyrolysis is shown in Fig. 1, and thus Ea and B can be obtained from this linear plot.

RESULTS AND DISCUSSION

1. Fuel Properties

Proximate and ultimate analyses of bean straw are shown in Table 1 along with calculated properties from the analyses. Volatile matter content of bean straw as received is about 83% (% of total weight as DAF basis). Since volatile matter is very sensitive to temperature, high volatile matter content means large amount of weight will be lost under high temperature in the torrefaction process. So it is important to keep the torrefaction temperature below T_{max} to avoid significant mass and energy loss.

2. Results of TGA Test

Fig. 2 shows the weight loss curves of the sample pyrolysis process, indicating that ~10% moisture existed in the fuel; pyrolysis was started at ~510 K at low heating rates (e.g., 10 and 20 K min⁻¹). The rapid pyrolysis zone occurred in the temperature range 520-700 K in which ~60% volatile matter was released; after the completion of the experiment, ~25% fixed carbon and ash were left. Moreover, with increasing heating rate, more material remained inside the fuel under the same temperature (e.g., <40% mass at β= 10 K min⁻¹, whereas >60% mass at β=80 K min⁻¹ remained in the fuel at 673 K), more time was required to heat the samples to the desired temperature under low heating rates, and volatile matter had longer time to be released from the fuels. Moreover, a low heating rate resulted in less temperature gradient inside the fuel samples which helps volatile matters to be liberated from the internal part of the fuel. The weight-loss rate curves of the bean straw at different heating rates are shown in Fig. 3. When the heating rate was increased from 10 to 80 K min⁻¹, T_{max} shifted to higher temperatures, and the maximum volatile release rate significantly increased and reached >50% min⁻¹ at a heating rate of 80 K min⁻¹. Yuan et al. also reported that the volatile release rate when pyrolyzing cattle manures increased with increasing heating rates [7]. According to Zheng et al. [34], hemicellulose was the most reactive to temperature and thermally degraded in the temperature range 500-590 K; cellulose degraded in the temperature range 600-670 K. Lignin, which
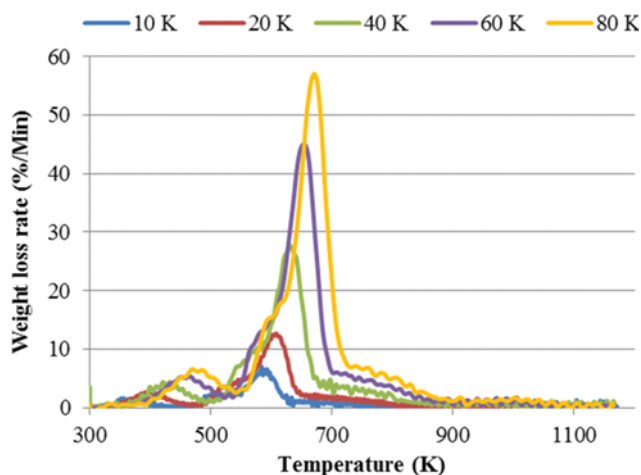
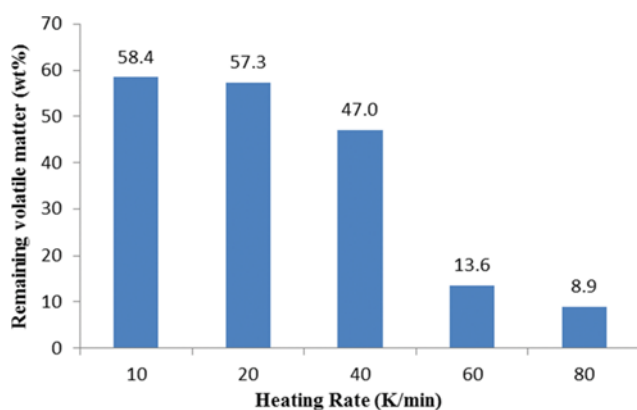**Fig. 3. TGA weight loss rate curves at various heating rates.**

Fig. 4. Remaining volatile matter (wt%) for different heating rates at peak temperature.

is more chemically complex, gradually degraded over a wide temperature from 443 to 1,173 K [34]. At higher heating rates, fuel samples absorbed more energy from the environment within the same period of time, triggering more reactions simultaneously, resulting in a rapid breakdown of molecular bonds inside hemicellulose, cellulose, and lignin. Thus, the release rate significantly increased. Fig. 4 gives the remaining volatile matter percentages inside the biomass at T_{max}, for different heating rates. It is seen that the remaining volatile matter percentage decreased with heating rate increasing, especially when heating rate elevated above 60 K min^{-1}. This is because with heat rate increasing T_{max} was shifted to higher temperature and larger heat flux (e.g. high heating rate) can break the fuel molecular bonds rapidly resulting in higher releasing rate and more volatile matter released from the fuel.

3. Chemical Kinetics

3-1. Chemical Kinetics of MVR-S

E and B were first calculated by the MVR-S method at five different heating rates, as shown in Fig. 5. E and B were in the ranges 80,000-112,000 kJ/kg (average value 98,158 kJ/kg and σ=7,340 kJ/kg) and 10 E+7-9.2 E+8, respectively. Moreover, both E and B generally increased with increasing heating rates, and the values only fluctuated at heating rate of 20 K min^{-1}. Similar phenomenon was
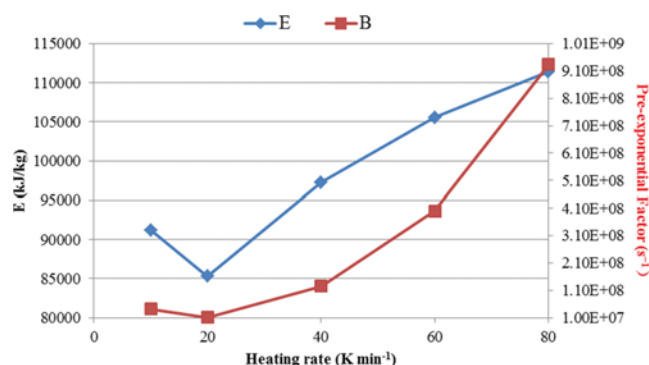

Fig. 5. Activation energies and pre-exponential factors.

Table 2. E and B values by different methods

Method	DAEM	MVR-M	MVR-S (40 K min^{-1})
E (kJ/kg)	1.58E+05	6.61E+04	9.73E+04
B (1/min)	1.67E+13	1.99E+05	1.25E+08

observed by Chen et al. and Mui et al. [35, 36]. Mui et al. explained that more reactions were simultaneously triggered at higher heating rates, causing a sharp rise in the reaction rates with more unstable radicals/intermediates resulting in amplified activation energy [36].

3-2. Chemical Kinetics of DAEM and MVR-M

To compare the chemical kinetics predicted by different methods, the values of E and B were also calculated by DAEM, MVR-M, and MVR-S methods (β=40 K min^{-1}) and are listed in Table 2. The chemical kinetics obtained from the DAEM was higher than that from MVR-S and MVR-M, especially the B value (1.67E+13), which is significantly higher than the values predicted by the other two methods. E of the bean straw was around 1.58E+05, which is very close to that of mesquite by the DAEM method (e.g., 1.57E+5 to 1.58E+5). It may be because biomass fuels have similar compositions (hemicellulose, cellulose, and lignin) and structure in the volatile matter. Among these compositions, hemicellulose and cellulose are both polymeric carbohydrate structures, while lignin is an amorphous cross linked resin of no distinct structure, which binds the fibrous cellulose particles [10]. Moreover, cellulose is a polymer, consisting of linear chains of glucopyranose units; hemicellulose is a complex polysaccharide mostly in cell wall structure; lignin is highly branched, substituted, mononuclear aromatic polymer in the cell walls for certain biomass [10]. These compositions of different biomass fuels have similar pyrolysis behaviors such as pyrolysis starting temperature although their weight percentages varied for different fuels [6].

4. Volatile Release Curve

4-1. Volatile Release Curves of MVR-S

By applying chemical kinetics to MVR-S, the simulated MVR-S weight loss curves at different heating rates were obtained and compared to the experimental data (Fig. 6). Among these curves, the curve at a heating rate of 40 K min^{-1} exhibits the least error for modeling the pyrolysis, especially in the range 500-660 K. At higher heating rates, the accuracy of the prediction curves decreased. For ex-
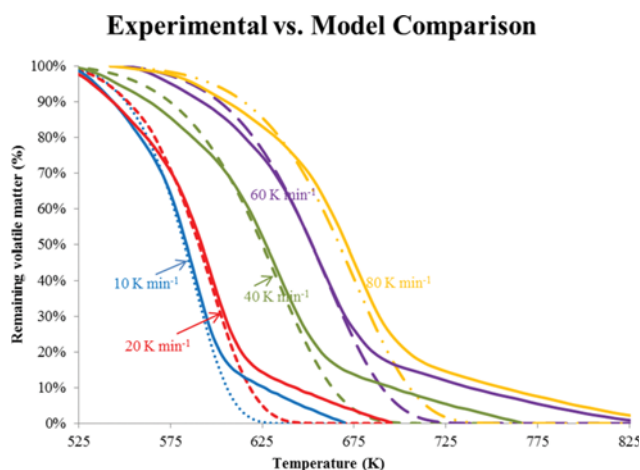
Fig. 6. Experimental data (solid line) and theoretical prediction (dash line) at different heating rates.

Table 3. Error analysis of the weight loss curves at different heating rates by MVR-S method

β (K min^{-1})	10	20	40	60	80
σ Root mean square error for whole domain of pyrolysis (%)	9.30	6.20	5.17	5.95	5.93
Maximum error (%) at a point	16.30	12.70	10.49	12.70	12.80

ample, the theoretical curves at heating rates of 60 K min^{-1} (purple solid and dash lines) and 80 K min^{-1} (yellow solid and purple lines) exhibited large error. The root mean square errors were 5.93% and 5.95% for heating rates of 60 K min^{-1} and 80 K min^{-1}, respectively, while it is only 5.17% for heating rate of 40 K min^{-1}.

4-2. Uncertainty Analysis of Weight Loss Curve of MVR-S

Table 3 lists the error analysis of the simulated curves by the MVR-S method at different heating rates, indicating that the simulated pyrolysis curves at heating rate of 40 K min^{-1} exhibited least root mean square error (5.17%), and the maximum error at a point was only 10.49%. Therefore, the kinetics obtained at a heating rate of 40 K min^{-1} was selected and compared to those obtained by the DAEM and MVR-M method. As a result, moderate heating rate is recommended for biomass pyrolysis studies.

4-3. Weight Loss Curves by Different Methods

Fig. 7 shows the comparison of the simulated weight loss curves by the DAEM, MVR-S, and MVR-M methods with the experimental data. As discussed before, DAEM is considered as an infinite number of complex reactions proceeding in parallel in the pyrolysis process. DAEM (the purple dash line) fitted the experimental data best for the entire pyrolysis domain, followed by MVR-M, and then MVR-S. MVR-S (the red dash line) agreed well with the experimental data at temperatures <820 K, whereas more deviations occurred with further increase in the temperature. Compared to the MVR-S, the result obtained by the MVR-M method (the green dash line) also showed a good agreement with the experimental data.
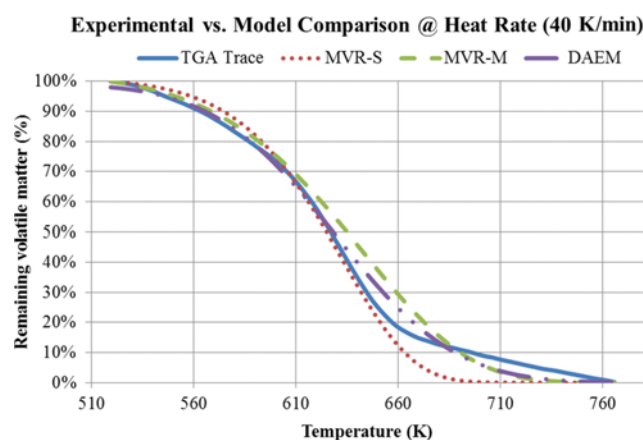
Fig. 7. Comparison of the model results (VM%) with the experimental data at heating rate 40 K/min.
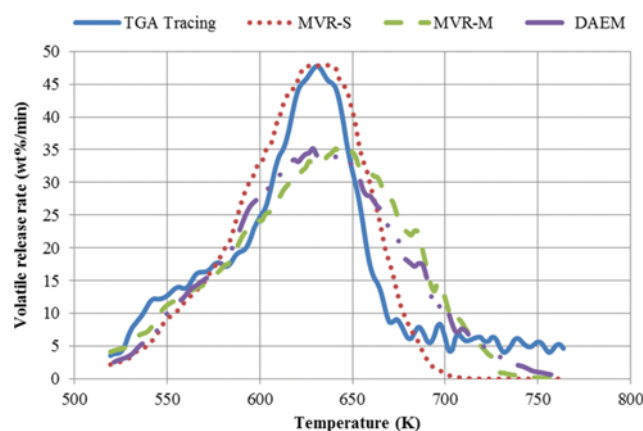

Fig. 8. Comparison of the experimental data for specific weight loss rate (% per min) versus temperature with different volatile release reaction models.

5. Volatile Release Rate Curves

5-1. Volatile Release Rate Curves of Different Methods

The volatile release rate is an important parameter in torrefaction process that affects the energy density of the final product. In this study, volatile release rates were predicted by the MVR-S, MVR-M, and DAEM methods, and the results were compared to the experimental data (Fig. 8). The MVR-S curve (the red dash line) shows a good agreement with the experimental volatile release rate in the entire pyrolysis domain and the peak point (e.g., the maximum volatile release rate point) also shows a good agreement, because B and E were selected to match the peak point of the experimental data in this method. The weight loss rate curves predicted by the DAEM and MVR-M methods presented similar deviations. DAEM and MVR-M overestimated the T_{max} and the maximum volatile release rates were under-predicted. As a result, these models were not as accurate as the MVR-S method at predicting volatile release rate and T_{max}. In torrefaction, temperatures <T_{max} and the volatile release rates below a certain level were recommended to avoid too much weight and energy loss. Even though DAEM can well predict the amount of volatile matter remaining in the fuel, it did not predict the release rate well, especially in the rapid pyroly-

Table 4. Error analysis of different models for fuel pyrolysis weight loss process

	DAEM	MVR-S	MVR-M
σ Root mean square error for whole domain of pyrolysis %	2.90	5.17	5.01
Maximum error (%) at a point	6.96	10.49	10.35

Table 5. Error analysis of different methods for predicting weight loss rate

Error	DAEM	MVR-S	MVR-M
σ Root mean square error for whole domain of pyrolysis %	6.13	5.60	7.79
Maximum error (%) at peak point	13.9	0	14.98

sis zone. Therefore, MVR-S method can be used to predict the upper limit temperature for the biomass torrefaction to obtain a high quality fuel.

5-2. Error Analysis of Different Methods

The error analysis of the different models for fuel pyrolysis of weight process is listed in Table 4. As discussed before, the DAEM predicted the weight loss behavior well, because the root mean square error of the entire pyrolysis domain and the maximum error at a point were only 2.9% and 6.96%, respectively, whereas the root mean square error and the maximum error at a point by the MVR-S and MVR-M methods were more than 5% and 10%, respectively. Therefore, DAEM can well predict the weight loss behavior, followed by MVR-M, and then MVR-S.

In addition to the weight loss process, an error analysis of the volatile release rate predictions of different methods was also conducted (Table 5). The root mean square error for the entire pyrolysis domain and the maximum error at the peak point by the MVR-S method were 5.60% and 0%, respectively, which are lower than those obtained by the other two methods. Particularly, at the peak point, error was zero by the MVR-S method, because the kinetics was selected to match the maximum volatile release rate, whereas DAEM and MVR-M methods exhibited >13% error. Thus, these two methods did not well describe the pyrolysis characteristics of bean straw.

6. Comparison of Different Methods

As discussed, DAEM accounts for different activation energies of the different chemical components within the bean straw. Thus, DAEM was more accurate in predicting the volatile matter weight loss process. However, chemical kinetics extracted from MVR-S and MVR-M were only based on a single point data or multiple-point data. These two methods do not fully represent the degree of heterogeneity of the fuel, which indicates the activation energy distribution. Therefore, more deviations in estimating weight loss process were observed. Similarly, MVR-S generated more errors than MVR-M (Table 4) in predicted weight loss process since it was simply based on a single point.

According to Yang et al., the peak mass loss rate for hemicellulose occurred at 540 K, and for cellulose occurred at 638 K; lignin was more difficult to decompose and its decomposition occurred

slowly over the whole temperature range. Lignin is full of aromatic rings with various branches, and the activity of the chemical bonds in lignin covered an extremely wide range [37]. The maximum mass loss rate of bean straw (occurred at around 630 K) may be mainly due to the decomposition of cellulose and some hemicellulose. Different from weight loss process, MVR-S exhibited better agreement with experimental data in estimating release rate, especially around the peak point, since E and B were extracted based on the peak point data. As noted, both DAEM and MVR-M underestimate the release rate around the peak point. These chemical kinetics did not well reflect thermal decomposition of cellulose and hemicellulose in the rapid release zone (600 K-650 K); they are more representing pyrolysis characteristics of the whole temperature domain. As a result, in order to better explore the mechanics of the volatile release rate, chemical kinetics such as activation energy of hemicellulose and cellulose as well as lignite and the weight percentage of each component of the bean straw need to be determined in the future.

CONCLUSIONS

Bean straw pyrolysis processes were conducted at different heating rates (10, 20, 40, 60, and 80 K min^{-1}). Chemical kinetics was extracted from the experimental data. The maximum volatile release methods including MVR-S and MVR-M as well as DAEM were developed to simulate the bean straw pyrolysis process, and the results obtained are as follows:

1. All these three methods (DAEM, MVR-M, and MVR-S) could be applied to study other biomass fuel pyrolysis characteristics. The maximum volatile release multiple point method was first time used to simulate the biomass pyrolysis process. It reasonably predicted the bean straw weight loss process and release rate.

2. In the MVR-S method, the activation energies and pre-exponents factors both increased when heating rates were increased from 10 to 80 K min^{-1}. The activation energies were in the range 80,000-112,000 kJ/kg (average value 98,158 kJ/kg and σ=7,340 kJ/kg). The simulated weight loss curve at a heating rate of 40 K min^{-1} showed the least error and was selected to compare with other methods.

3. For the simulated weight loss curves, the DAEM fitted the experimental data best, followed by MVR-M, and then MVR-S. As a result, the DAEM is recommended for predicting the biomass volatile pyrolysis weight loss process. For the volatile release rate, the MVR-S method well predicted the release rate of the entire pyrolysis domain, especially at the peak point, whereas the DAEM and SRM-M methods exhibited more deviations for entire domain and the peak point.

4. Chemical kinetics extracted form MVR-S method well described characteristics of volatile matter release rate. It could be recommended to predict fuel torrefaction volatile release rate and upper limit temperature of torrefaction. Compared to MVR-S, both the DAEM and MVR-M overestimated the T_{max} and underestimated the volatile release rate in the rapid pyrolysis zone.

NOMENCLATURE

E   : activation energy
DAEM   : distributed activation energy model
MVR   : maximum volatile release
MVR-S   : maximum volatile release-single point
MVR-M   : maximum volatile release-multiple points
B   : pre-exponential factor
TGA   : thermogravimetric analysis

REFERENCES

1. W. Chen, *Fixed bed counter current low temperature gasification of mesquite and juniper biomass using air-steam as oxidizer*, PhD dissertation, Mechanical Engineering, Texas A&M University, College Station (2012).

2. G. Gordillo, K. Annamalai and N. Carlin, *Renewable Energy*, **34**, 2789 (2009).

3. A. Anca-Couce, A. Berger and N. Zobel, *Fuel*, **123**, 130 (2014).

4. S. Chayaporn, P. Sungsuk, S. Sunphorka, P. Kuchonthara, P. Piumsomboon and B. Chalermsinsuwan, *Korean J. Chem. Eng.*, **32**, 1081 (2015).

5. R. Soysa, Y. S. Choi, S. K. Choi, S. J. Kim and S. Y. Han, *Korean J. Chem. Eng.*, **33**, 603 (2016).

6. W. Chen, S. S. Thanapal, K. Annamalai, D. Ranjan, B. Lawrence and R. J. Ansley, *Kinetics of Pyrolysis of Mesquite Fuel: Comparison of Different Methods*, ASME Turbo Expo 2014: Turbine Technical Conference and Exposition, 3A, V03AT03A022 (2014).

7. H. Cao, Y. Xin, D. Wang and Q. Yuan, *Bioresour. Technol.*, **172**, 219 (2014).

8. M. Jeguirim, J. Bikai, Y. Elmay, L. Limousy and E. Njeugna, *Energy for Sustainable Development*, **23**, 188 (2014).

9. Y. F. Huang, P. T. Chiueh, W. H. Kuan and S.L. Lo, *Appl. Energy*, **110**, 1 (2013).

10. S. A. El-Sayed and M. E. Mostafa, *Energy Convers. Manage.*, **85**, 165 (2014).

11. T. Sonobe and N. Worasuwannarak, *Fuel*, **87**, 414 (2008).

12. K. Q. Tran, Q. V. Bach, T. T. Trinh and G. Seisenbaeva, *Appl. Energy*, **136**, 759 (2014).

13. C. R. Cardoso, M. R. Miranda, K. G. Santos and C. H. Ataíde, *J. Anal. Appl. Pyrol.*, **92**, 392 (2011).

14. M. J. Antal and G. Varhegyi, *Ind. Eng. Chem. Res.*, **34**, 703 (1995).

15. L. Sørum, M. Grønli and J. E. Hustad, *Fuel*, **80**, 1217 (2001).

16. J. Caia, W. Wu and R. Liua, *Renewable Sustainable Energy Reviews*, **36**, 236 (2014).

17. A. Soria-Verdugo, N. Garcia-Hernando, L. M. Garcia-Gutierrez and U. Ruiz-Rivas, *Energy Convers. Manage.*, **65**, 239 (2013).

18. G. J. Pitt, *Fuel*, **41**, 267 (1962).

19. D. B. Anthony, H. C. Howard, H. C. Hottel and H. P. Meissner, *Symposium (International) on Combustion*, **15**, 1303 (1974).

20. B. Martin, *Pyrolysis and ignition of behavior of coal, cattle biomass, and coal/cattle biomass blends*, Texas A&M University, M.S. Thesis (2006).

21. M. Güneş and S. K. Güneş, *Energy Sources*, **30**, 1460 (2008).

22. B. Caprariis, P. Filippis, C. Herce and N. Verdone, *Energy Fuels*, **26**, 6153 (2012).

23. A. Soria-Verdugo, E. Goos and N. García-Hernando, *Fuel Processing Technol.*, **134**, 360 (2015).

24. K. Kirtania and S. Bhattacharya, *Bioresour. Technol.*, **107**, 476 (2012).

25. P. Tiwari and M. Deo, *AIChE J.*, **58**, 505 (2012).

26. C. Tangsathitkulchai, S. Junpirom and M. Tangsathitkulchai, *Korean J. Chem. Eng.*, **27**, 791 (2010).

27. J. Cai, W. Wu and R. Liu, *Bioresour. Technol.*, **132**, 423 (2013).

28. R. L. Braun and A. K. Burnham, *Energy Fuels*, **1**, 153 (1987).

29. A. K. Burnham, *Chem. Eng. J.*, **108**, 47 (2005).

30. T. Mani, P. Murugan and N. Mahinpey, *Ind. Eng. Chem. Res.*, **48**, 1464 (2009).

31. J. Cai and R. Liu, *Bioresour. Technol.*, **99**, 2795 (2008).

32. J. Cai, F. He and F. Yao, *J. Mathematical Chemistry*, **42**, 949 (2006).

33. K. Annamalai and I. K. Puri, *Combustion Science and Engineering*, Taylor & Francis Group (2007).

34. H. Yang, R. Yan, H. Chen, D. Lee and C. Zheng, *Fuel*, **85**, 1781 (2007).

35. D. Chen, J. Zhou and Q. Zhang, *Bioresour. Technol.*, **169**, 313 (2014).

36. E. L. K. Mui, W. H. Cheung, V. K. C. Lee and G. McKay, *Ind. Eng. Chem. Res.*, **47**, 5710 (2008).

37. H. Yang, R. Yan, H. Chen, D. H. Lee and C. Zheng, *Fuel*, **86**, 1781 (2007).